

# Modeling Dynamical Influence in Human Interaction Patterns

Wei Pan, Manuel Cebrian, Wen Dong, Taemie Kim  
and Alex Pentland  
*The Media Laboratory*  
*Massachusetts Institute of Technology*

## Abstract

We present a new perspective, together with a model and algorithm, on a well-observed property of many social phenomena: the influence strength between individuals changes over time (e.g., friendships break and reform). We propose an unsupervised generative switching model that simultaneously captures the system dynamics as the outcome of both (i) the influence between individuals (each modeled as an HMM), and (ii) the dynamics of the influence itself. We describe here a variational Expectation-Maximization (EM) algorithm. In our experiments, we illustrate applications of detecting structural change, predicting turn taking by analyzing a real group discussion behavior dataset and understanding flu influence patterns between US states. Results demonstrate that our approach is a strong alternative for modeling complex interacting social systems.

## 1 Introduction

Our model tackles the problem of analyzing and understanding *who influences whom* in a social system, such as a group discussion process, which has been an interesting question for social scientists for the last six decades [1]. Influence is also interesting in the context of leadership where the influence between one another has been recognized as a significant factor of group performance [2]. In this paper, we handle this problem by modeling each individual in a social system as an HMM, and all HMMs interact with each other according to a family of influence matrices that describe different interaction patterns. The system then switches between different influence matrices over time.

In the prevailing studies on social computing, quantitative efforts have focused on the *static* picture of the influence [3] [4], namely who is influencing whom in a social system when longitudinal data on human interactions is aggregated in a snapshot. However, there is extensive evidence leading us to think that influence is indeed a dynamical process[5][6]. Therefore, we believe that, in a social system such as a group discussion session, the influence between subjects fluctates as well and a better model should take the dynamics of influence itself into consideration (i.e. how person A influenced person B at time  $t$  versus the same question at a different moment in the future).

Our approach is in essence a switching version of influence model [7], a special type of Bayesian network. We are interested in the challenge of inferring influence and learning parameters in a social system based solely on individual observations over time, i.e., without actually knowing the individual interaction patterns. We define influence between two nodes as the conditional probability between the internal states of these two nodes in consecutive time frames. We approach the problem of dynamical influence by introducing a set of different influence matrices, which captures the different ways individuals interact over time. A latent trace  $r_t$  is included also to represent the index of the current active influence matrix at time  $t$ .  $r_t$  is treated as a stochastic process as well. Therefore, our model not only captures the dynamics of individual behaviors, but also the underlying latent variables tracing the dynamics of influence. It should be noted that in our approach system dynamics and influence dynamics are learned simultaneously in a unified framework, and the learning algorithm is unsupervised.

## 2 Related Work

The Bayesian network is a tool often used in understanding patterns in social interactions [8] [7]. Earlier projects have used coupled HMM [3], and more recent projects have used the influence model [9], dynamic system trees [9] and interacting Markov chains [10]. All these approaches lack the ability to track the changing influence in real social systems.

Other relevant general multi-dimensional time series approaches such as LDS [11] and the prototype model [12] are not able to recognize the network structure and weights on edges between nodes in social systems.

The classical method for Bayesian network inference is the junction tree algorithm [13], of which the complexity increases exponentially to the number of chains. Here we demonstrate a variational approach with polynomial time complexity. The accuracy of this type of approach has been satisfactory in other applications [14] [15] [7].

We are fully aware of the class of time-varying models: from EGRM [16] to TESLA [17], to name two. We model the dynamics of every node and edge in a network instead of feature functions as in EGRM. Our work is also significantly different from TESLA: We consider changing influence, which are continuous real values, as the topological dynamics, and our generative model captures the interaction of nodes and the dynamics of the interaction strength simultaneously.

## 3 Our Model

### 3.1 Model Description

Our approach, the Dynamical Influence Process, is a switching extension to the existing influence model [9]. It is composed of  $C$  interacting chains. In this model, similar to an HMM, each chain  $c \in \{1, \dots, C\}$  takes one of a finite number of latent states at any discrete time  $t$ :  $h_t^{(c)} \in \{1, \dots, S\}$ . Corresponding to each latent state  $h_t^{(c)}$ , we

observe  $O_t^{(c)}$  which follows a conditional probability distribution  $\text{Prob}(O_t^{(c)}|h_t^{(c)})$ , usually known as the emission probability in HMM literature. In practice, it can either be multinomial for discrete observations or Gaussian mixture for continuous observations.

We proceed to describe the cross-chain interactions of this system.  $\mathbf{M}_{i,j}$  denotes the  $i$ th row and  $j$ th column of matrix  $\mathbf{M}$  in the following discussion. In this model, we have  $J$  different interaction configurations described by matrices  $\mathbf{R}^1, \dots, \mathbf{R}^J$  and only one configuration  $r_t \in \{1, \dots, J\}$  is active at time  $t$ .  $J$  is a hyper-parameter set by the user, and we will cover the detail of selecting the values of hyper-parameters in the experiment section. The model changes its interaction configurations  $\{r_t\}_{t=1,2,\dots}$  slowly with respect to the sampling period according to the following Markov prices:

$$r_{t+1}|r_t \sim \text{multi}(V_{r_t,1}, \dots, V_{r_t,J}), \quad (1)$$

where  $\mathbf{V}$  is constrained by another hyper-parameter  $p^V, p^V > 0$ . A large  $p^V$  will ensure that our model switch slowly to other influence configurations and tend to remain in the current configuration:

$$(V_{r_t,1}, \dots, V_{r_t,J}) \sim \text{Dirichlet}(10^0, 10^0, \dots, 10^{p^V}, \dots, 10^0). \quad (2)$$

$$\begin{matrix} \uparrow & \uparrow & \dots & \uparrow & \dots & \uparrow \\ 1, & 2, & \dots, & r_t, & \dots, & J \end{matrix}$$

Given that the interaction configuration  $r_t$  is in effect, the latent state of chain  $c$  in this system at time  $t + 1$  is determined by another random chain  $q_t^{(c)} \in \{1, \dots, C\}$  according to a multinomial distribution described by the configuration matrix  $\mathbf{R}^{r_t}$ . This is similar to mixture models such as the Gaussian mixture model [18]:

$$q_t^{(c)}|r_t \sim \text{multi}(\mathbf{R}_{c,1}^{r_t}, \dots, \mathbf{R}_{c,C}^{r_t}). \quad (3)$$

The state of chain  $c$  at  $t + 1$  thus is determined by:

$$h_t^{(c)}|h_{t-1}^{(1)}, \dots, h_{t-1}^{(C)}, q_t^{(c)} = c' \sim \begin{cases} \text{multi}(\mathbf{E}_{h_t^{(c)},1}^{(c)}, \dots, \mathbf{E}_{h_t^{(c)},S}^{(c)}) & c' = c \\ \text{multi}(\mathbf{F}_{h_t^{(c')},1}^{(c')}, \dots, \mathbf{F}_{h_t^{(c')},S}^{(c')}) & c' \neq c \end{cases}. \quad (4)$$

Eq. 3 and Eq. 4 define the concept of influence: the state of a chain is "influenced" by states of all chains. Given the model description, the likelihood function is

$$\mathcal{L}(O, h, q, r|\mathbf{E}, \mathbf{F}, \mathbf{R}, \mathbf{V}) \quad (5)$$

$$= \prod_{t=2}^T \left\{ \text{Prob}(r_t|r_{t-1}) \prod_{c=1}^C \left[ \text{Prob}(O_t^{(c)}|h_t^{(c)}) \text{Prob}(h_t^{(c)}|h_{t-1}^{(1,\dots,C)}, q_{t-1}^{(c)}) \text{Prob}(q_t^{(c)}|r_t) \right] \right\}$$

$$\times \prod_{c=1}^C \text{Prob}(O_1^{(c)}|h_1^{(c)}) \text{Prob}(h_1^{(c)}) \text{Prob}(r_1). \quad (6)$$

Our model is illustrated in Fig. 1.

In contrast to the static influence process [4], the influence between different parts in the system is no longer static, but evolves slowly according to a Markov process. As can be seen in our experiment, this is indeed the case of a real social system.

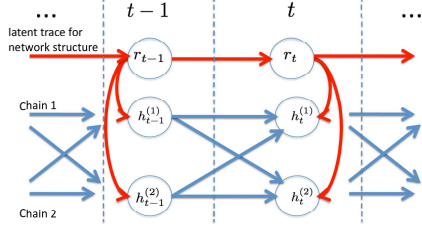


Figure 1: A graphical representation of our model when  $C = 2$ .

### 3.2 Model Learning

Here we show key steps for our variational E-M algorithm. Definition is denoted by  $\equiv$ , and  $\sim$  denotes the same distribution but the right side should be normalized accordingly. We refer to our supplementary materials for full details.

### 3.3 E-Step

We adopt a procedure similar to the forward-backward procedure in HMM literature. We compute the following forward parameters for  $t = 1, \dots, T$ :

$$\alpha_{t,c}^{r_t} \equiv \text{Prob}(h_t^{(c)} | r_t, O_{1:t}), \quad (7)$$

$$\kappa_t \equiv \text{Prob}(r_t | O_{1:t}), \quad (8)$$

where  $O_{1:t}$  denotes  $\{O_{t'}^{(c)}\}_{t'=1, \dots, t}^{c=1, \dots, C}$ . However, exact inference is not tractable. We adopt the variational approach in [14][19], and E-M is still guaranteed to converge under variational approximation[19]. We proceed to decouple the chains by:

$$\text{Prob}(h_t^{(1)}, \dots, h_t^{(C)} | O_{1:t}, r_t) \approx \prod_c Q(h_t^{(c)} | O_{1:t}, r_t), \quad (9)$$

and naturally:

$$\alpha_{t,c}^{r_t} \approx Q(h_t^{(c)} | O_{1:t}, r_t) \quad (10)$$

Using the same idea, we can compute the following backward parameters for all  $t$ :

$$\beta_{t,c}^{r_t} \equiv \text{Prob}(h_t^{(c)} | r_t, O_{t:T}), \quad (11)$$

$$\nu_t \equiv \text{Prob}(r_t | O_{t:T}). \quad (12)$$

### 3.4 M-step

With  $\kappa_t$  and  $\nu_t$ , we can estimate:

$$\xi_{i,j}^t \equiv \text{Prob}(r_t = i, r_{t+1} = j | O_{1:T}) = \frac{\text{Prob}(r_t = i | O_{1:t}) \text{Prob}(r_{t+1} = j | O_{t+1:T}) \text{Prob}(r_{t+1} | r_t)}{\sum_{i,j} \text{Prob}(r_t = i | O_{1:t}) \text{Prob}(r_{t+1} = j | O_{t+1:T}) \text{Prob}(r_{t+1} | r_t)}, \quad (13)$$

$$\lambda_i^t = \text{Prob}(r_t = i | O_{1:T}) = \frac{\sum_j \xi_{i,j}^t}{\sum_i \sum_j \xi_{i,j}^t}, \quad (14)$$

and update  $V$  by:

$$\mathbf{V}_{i,j} \leftarrow \frac{\sum_t \xi_{i,j}^t + k}{\sum_t \sum_j \xi_{i,j}^t + p^V}, \quad (15)$$

where  $k = p^V$  if  $i = j$ , 0 otherwise.

We continue to compute the joint distribution  $\text{Prob}(h_t^{(c)}, h_{t+1}^{(c)}, q_{t+1}^{(c)}, r_{t+1} | O_{1:T})$ , and update parameters  $\mathbf{R}$ ,  $\mathbf{E}$  and  $\mathbf{F}$  by marginalizing this joint distribution. Please refer to the supplementary material for detail.

## 4 Toy Example

In this toy example, we demonstrate how our algorithm can be applied to find structural changes in network dynamics. From a dynamical influence process composed of two interacting HMM chains, we sample two binary sequences of 600 time steps. The data are shown in Table 1 (left). Each chain has two hidden states with a random transition biased to remaining in the current state. To simulate a switch in influence dynamics, we sample with configuration  $\mathbf{R}^1$  (shown in Table 1) in the first 200 frames, and later on we sample with configuration  $\mathbf{R}^2$ . We purposely make the two configuration matrices different from each other.  $\mathbf{E}^{(c)}$  and  $\mathbf{F}^{(c)}$  are randomly generated for this process. All parameters are initialized randomly.

Table 1: Left: Part of the two input toy sequences for a two-chain dynamical influence process. Right: The original two influence matrices of the toy model and the same matrices learned by our algorithm with  $J = 3$  and  $p^V = 10^1$ .

SEQ. NO.	DATA(PARTIALLY)		$\mathbf{R}^1$	$\mathbf{R}^2$
1	221111121212212...	True	$\begin{pmatrix} 0.90 & 0.10 \\ 0.10 & 0.90 \end{pmatrix}$	$\begin{pmatrix} 0.05 & 0.95 \\ 0.95 & 0.05 \end{pmatrix}$
2	112111212121122...	Learned	$\begin{pmatrix} 0.93 & 0.07 \\ 0.10 & 0.89 \end{pmatrix}$	$\begin{pmatrix} 0.08 & 0.92 \\ 0.94 & 0.06 \end{pmatrix}$

**Choosing Hyper-Parameters:** We now discuss the selection of hyper-parameters  $J$  and  $p^V$ . For the number of active configuration matrices  $J$ , we here illustrate its characteristics by running the same example with  $J = 3$ . We show the poster distribution of  $r_t$  (calculated in Eq. 33) in Fig. 2(a). Our algorithm discovers the sudden change of influence weights accurately at  $t = 200$ . In addition, we discover that since the toy process only has two true configuration matrices, the posterior probability of the 3rd configuration being active is almost zero for any  $t$ . The system properties are fully captured by the other two configuration matrices during the training. The learned

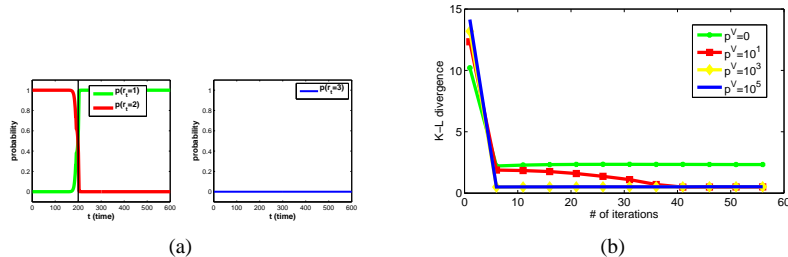


Figure 2: (a): The posterior of  $r_t$  given observations is shown above when  $J = 3$  at convergence. The middle black vertical line on the left indicates the true structural change (i.e.  $\mathbf{R}^1$  is replaced by  $\mathbf{R}^2$  during sampling). (b): The K-L divergence between learned parameters and the true distributions with respect to number of iterations.

configuration matrices (shown in Table 1) are correctly recovered. Based on Fig. 2(a) and experiments with other values for  $J$  (which we can not show here due to the space limitation), we conclude that readers should gradually increase  $J$  until the newly added configuration matrices are no longer useful in capturing additional dynamical information from the data, by ensuring there is no constant zero posterior probability as in the right plot in Fig. 2(a).

We demonstrate convergence of the K-L Divergence between the true distributions of the transition probability and the learned distributions in Fig. 2(b) with different values of  $p^V$ . As can be seen in Fig. 2(b), the algorithm converges quickly within 50 iterations. We discover that when  $p^V$  is small, we may encounter over-fitting where the learned model rapidly switches between different configurations to best suit the data. Therefore, in Fig. 2(b), the divergence for  $p^V = 0$  remains higher than other  $p^V$  values at convergence. In conclusion, we advise users to increase  $p^V$  gradually until the posterior of  $r_t$  does not fluctuate.

## 5 Experiments on Human Interaction Data

### 5.1 Dataset Description and Preprocessing

The dataset used in this experiment comes from a group discussion experiment in [20]. Researchers in [20] recruited 40 groups with four subjects in each group for this experiment. During the experiment, each subject was required to wear the sociometric badge on their necks for audio recording, and each group was required to perform two different group discussion tasks: a brainstorming task and a problem solving task. Each task usually lasted for 3 to 10 minutes. We kindly refer readers to the original paper for details on data collection and experiment preparations.

The groups were asked to perform these tasks in two different settings: (a) being *co-located* in the same room around a table and (b) being *distributed* in two rooms with only audio communication being available between the pairs. (The badge is deployed in both cases for audio collecting.) Later in the paper we refer to these two settings

as CO and DS respectively. Since discussions are held in four-person groups, each sample for a discussion session is composed of four sequences collected by the four badges on participants’ chests. The audio sequence picked up by each badge is split into one-second blocks. Variances of speech energy are calculated for each block. We then applied a hard threshold to convert them into binary sequences. In all experiments, we only use binary sequences as data input.

## 5.2 Predicting Turn Taking in Discussion

One important aspect of modeling interaction dynamics is the ability to predict turn taking—who will speak next in the interaction process. We here explain an application of our dynamical influence process to predict turn taking, and we show that it is possible to achieve good accuracy in prediction given only the binary audio volume variance observations, with no information from the audio content.

We separate all samples into four categories according to their original context and content, and each category is explained in Table 2. All audio data are converted into binary sequences with the procedure described in the beginning of this section. We end up with 44 samples, and each of them is composed of four sequences from all four subjects in the group. Ten occurrences of turn taking behavior from each sample are selected for prediction purposes.

Two prediction methods are implemented and evaluated: a) the dynamical influence model; b) the TESLA-based prediction (using the implementation from the authors in [21]) and c) the nearest-neighbor (NN) approach.

In the dynamical influence model, we train all parameters using the data before  $t$  to predict the turn taking behavior at  $t$ . Each chain in our model, which represents one person in the group, has two hidden states. The emission probability is learned by the E-M inference algorithm in this example. Since our algorithm is a generative process, we sample time  $t$  from our model, and mark the chain that changes the most toward the high-variance observational state as the turn taker.

For TESLA, we use the official implementation to obtain the dynamical weights between pairs of nodes, and we pick the node which has the strongest correlation weight to other nodes at  $t - 1$  as the turn taker at  $t$ . We tried different ways of using the output from TESLA for prediction, and we manually tuned hyper parameters. In this paper we report the best results we are able to obtain using TESLA.

To predict the turn taking at time  $t$  using the nearest neighbor method, we look over all previous instances of turn taking behaviors that have the same speaker as the one in  $t - 1$ , and predict by using the most frequent outcomes.

The accuracy for each algorithm is listed in Table 3. We also show the prediction accuracy for the half of all samples that have more complex interactions, i.e., higher entropy. For our dynamical influence based approach, we list error rates for  $J = 1, 2$  and 3. We notice that our algorithm outperforms others in all categories with different  $J$ . Because people are likely to form and reform different sub groups in brainstorming sessions, larger  $J$  becomes necessary to capture the dynamics of brainstorming tasks as shown in the DS+BS column in Table 3. This performance is quite good considering that we are using only volume and that a human can only predict at around 50% accuracy for similar tasks[22].

Table 2: The description for four different categories of all the samples.

CATEGORY	TASK DESCRIPTION
CO+PS	Four people perform a problem solving task in the same room.
CO+BS	Four people perform a brainstorming session in the same room.
DS+PS	Four people perform the same problem solving task in two rooms with Skype.
DS+BS	Four people perform the same brainstorming session in two rooms with Skype.

Table 3: Accuracy for different turn taking prediction methods on both the full dataset and the half of the dataset with more complex interactions. The random guess accuracy is 33%. Human accuracy is typically around 50% for similar tasks[22].

METHODS	ACCURACY ALL SAMPLES				ACCURACY COMPLEX INTERACTION SAMPLES			
	DS+BS	DS+PS	CO+BS	CO+PS	DS+BS	DS+PS	CO+BS	CO+PS
TESLA	0.41	0.42	0.32	0.25	<b>0.64</b>	0.47	0.44	0.21
NN	<b>0.58</b>	0.60	0.48	0.50	0.47	0.47	0.38	0.26
Ours(J=1)	0.45	<b>0.67</b>	<b>0.75</b>	<b>0.63</b>	0.56	0.77	0.73	<b>0.61</b>
Ours(J=2)	0.46	0.58	0.65	0.34	0.56	0.72	<b>0.78</b>	0.50
Ours(J=3)	0.50	0.60	0.55	0.48	0.56	<b>0.94</b>	0.65	0.56

More importantly, our model seems to perform much better than the competing methods for more complex interactions. For simple interactions, it seems that  $J = 1$  or even NN perform the best due to the fact that there is little shift in influence structure during the discussion. However, when handling complex interaction processes, the introduction of a switching influence dynamics dramatically improves the performance as shown in Table 3. Our results strongly suggest that the dynamical influence assumption in our model is reasonable and necessary in modeling complex group dynamics, and it can vastly improve prediction accuracy. However, in simple cases, the model achieves the highest performance only when  $J = 1$ , i.e. the influence is static.

### 5.2.1 Discussion on Other Time-varying Network Algorithms

TESLA fails in most prediction tasks, and we believe that the formulation of TESLA doesn't suit our applications, because it only captures the correlations between observations from dyad nodes at each time step and models the process as a time-varying network. We speculate that similar discriminative approaches adopted in [16] may not be suitable for our applications either. *It can be concluded that while time-varying models provide valuable information on network structural changes, the dynamics of influence and interaction in social systems are different from dynamics of network structures.* Our generative model, on the other hand, becomes a new effective and competitive perspective for such applications.

## 6 Modeling Flu Epidemics as Influence Dynamics

In this experiment, we demonstrate that flu spreading can be modeled as the outcome of interaction between people living in different regions in US.

We apply our algorithm to the weekly US flu activity data from Google Flu Trend [23]. All 50 states in US are divided into ten regions by their geo-location. We model each region as one chain in our dynamical influence model. As the data is continuous, six hidden states are used for each chain, and we choose Gaussian distribution as the emission distribution. We set the emission probability distribution to be the same for each chain and keep it fixed during the learning process so that the same hidden states for each chain share the same semantic meaning. The first 290 weeks (from 2003 to early 2009) are used for training and the remaining for testing. We set  $J = 3$ ,  $p^V = 10^{-1}$  for optimized performance.

We show the posterior for  $r_t$  in Fig. 3 after our model converges with the training data. While there are many small peaks suggesting changes in influence, the probability changes dramatically around Christmas, which suggests that the influence patterns among these ten regions are very different during the holiday season. Our algorithm actually reveals Christmas traveling by looking at only flu data in a fully unsupervised manner.

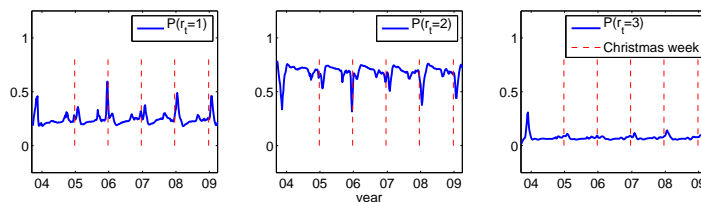


Figure 3: The inferred posterior for  $r_t$  given all observations after convergence is shown here. While there are many small peaks indicating changes in influence, the largest peaks occur at Christmas holiday seasons, which implies that influence between states are very different in Christmas holidays comparing with other dates. This matches the common sense that travelling patterns are different around holiday seasons. In our experiment, we find that three configuration matrices are good enough to capture the flu dynamics.

We proceed to study the long-term prediction abilities of different models. The prediction error results are shown in Table 4. We compare with different approaches in predicting flu data: the Linear Dynamical System(LDS) (based on a modern implementation [24]), our approach with  $J = 3$ , and ours with  $J = 1$  (the influence model). As a benchmark, we also show the results of predicting flu using the average value of the historical flu data of the same date. For our model, when predicting at  $t$ , we use a configuration matrix  $\mathbf{R} = a_t^1 \mathbf{R}_1 + \dots + a_t^J \mathbf{R}_J$ , where  $a_t^j$  is  $\text{Prob}(r_{t'} = j | \text{training data})$ , and  $t'$  denotes the same date of  $t$  in the previous year. Prediction is done by sampling our generative model with trained parameters and estimating expectations as the prediction.

The flu data in 2009 is very different from previous years. However, as we anticipated, people still maintain similar traveling routines, and our model captures the underlying influence dynamics rather than the raw prototype of flu seasonal patterns. Therefore, our model prediction is better than using the historical data directly as illustrated in Fig. 4.

Our approach performs better when  $J = 3$ , which verifies our assumption that the dynamics of the influence patterns are very important to prediction accuracy. As for LDS, the performance is unsatisfactory. We believe that the complicated nature of the system is unlikely to be captured by a linear approach such as LDS.

There are several high performance flu prediction models that offer comparable performance. However, our work reveals one novel perspective that the dynamics of flu spreading can be modeled partially by the influence between states and the changes of the influence itself. In particular, the influence dynamics learned by our model correlate well with the holiday seasons, which strongly suggests that the influence dynamics learned in our model are indeed capturing real interaction dynamics among US states.

We present another application of detecting influence structural change with the same group discussion dataset in the supplementary material.

Table 4: This table shows accumulated square error for different algorithms in predicting weekly flu epidemic from April, 2009 to August, 2009.

<b>METHOD</b>	<b>ERROR (RESCALED)</b>
Historical Data	3.44
LDS	5.41
Our Approach (J=1)	1.38
Our Approach (J=3)	<b>1.18</b>

## 7 Conclusions

We have developed an unsupervised generative model that captures the system dynamics as the outcome of both the influence between individuals and the dynamics of influence. Our model directly tackles the important sociological question of analyzing who influence whom in social systems. In our model,  $C$  HMM chains interact with each other according to a family of influence matrices describing different interaction patterns, and switch between them over time. A fast variational inference scheme is also developed to handle large system such as the flu epidemic in US. We have demonstrated the performance of our model in applications of detecting structural change, predicting turn taking and understanding epidemic dynamics. Our model provides a new perspective for modeling dynamics in network structures and influence structures.

Our model provides a rich understanding of patterns of influence in social groups, and in future works we can leverage such information to provide benefit to the groups themselves. As group dynamics have a strong relationship with the group's performance [25], there have been efforts to measure the communication patterns and provide feedback to the group in real-time [20, 26]. Our approach can enable such feedback

specific to influence structures which may lead to more effective leadership, stronger ties among group members and higher performance of teams.

Our immediate next step is also to apply our approach to larger and longer individual human behavioral datasets which we are currently collecting. This would fully leverage our fast inference scheme, because the current interest in computational social science is in the scale of thousands of individuals [27]. This would also allow us to leverage the power of machine learning to reach a better understanding of changes in human interaction patterns, and make significant quantitative contributions to social science.

## References

- [1] E. Katz and P.F. Lazarsfeld. *Personal influence*. Free Pr., 1955.
- [2] G.F. Farris and F. Lim. Effect of performance on leadership, cohesiveness, influence, satisfaction and subsequent performance. *Journal of Applied Psychology*, 53(6):490–497, 1969.
- [3] M. Brand, N. Oliver, and A. Pentland. Coupled hidden Markov models for complex action recognition. In *IEEE Computer Society Conference on Computer Vision and Pattern Recognition*, pages 994–999, 1997.
- [4] W. Dong and A. Pentland. Modeling influence between experts. *Lecture Notes in Computer Science*, 4451:170, 2007.
- [5] S.A. Ansari, V.S. Springthorpe, and S.A. Sattar. Survival and vehicular spread of human rotaviruses: possible relation to seasonality of outbreaks. *Reviews of infectious diseases*, 13(3):448–461, 1991.
- [6] J.P. Onnela, J. Saramaki, J. Hyvonen, G. Szabó, D. Lazer, K. Kaski, J. Kertész, and A.L. Barabási. Structure and tie strengths in mobile communication networks. *Proceedings of the National Academy of Sciences*, 104(18):7332, 2007.
- [7] W. Dong, B. Lepri, A. Cappelletti, A.S. Pentland, F. Pianesi, and M. Zancanaro. Using the influence model to recognize functional roles in meetings. In *Proceedings of the 9th international conference on Multimodal interfaces*, pages 271–278. ACM, 2007.
- [8] T. Choudhury and S. Basu. Modeling conversational dynamics as a mixed memory markov process. In *Proc. of Intl. Conference on Neural Information and Processing Systems (NIPS)*. Citeseer, 2004.
- [9] S. Basu, T. Choudhury, B. Clarkson, A. Pentland, et al. Learning human interactions with the influence model. *MIT Media Laboratory Technical Note*, 2001.
- [10] D. Zhang, D. Gatica-Perez, S. Bengio, and D. Roy. Learning Influence Among Interacting Markov Chains. 2005.
- [11] E. B. Fox, E. B. Sudderth, M. I. Jordan, and A. S. Willsky. Nonparametric Bayesian learning of switching linear dynamical systems. In *Neural Information Processing Systems 21*. MIT Press, 2009.
- [12] W. Pan and L. Torresani. Unsupervised hierarchical modeling of locomotion styles. In *Proceedings of the 26th Annual International Conference on Machine Learning*. ACM New York, NY, USA, 2009.
- [13] M.I. Jordan. *Learning in graphical models*. Kluwer Academic Publishers, 1998.

- [14] R.J. Weiss and D.P.W. Ellis. A variational EM algorithm for learning eigenvoice parameters in mixed signals. In *Proceedings of the 2009 IEEE International Conference on Acoustics, Speech and Signal Processing-Volume 00*, pages 113–116. IEEE Computer Society, 2009.
- [15] Z. Ghahramani and M.I. Jordan. Factorial hidden Markov models. *Machine learning*, 29(2):245–273, 1997.
- [16] F. Guo, S. Hanneke, W. Fu, and E.P. Xing. Recovering temporally rewiring networks: A model-based approach. In *Proceedings of the 24th international conference on Machine learning*, page 328. ACM, 2007.
- [17] A. Ahmed and E.P. Xing. Recovering time-varying networks of dependencies in social and biological studies. *Proceedings of the National Academy of Sciences*, 106(29):11878, 2009.
- [18] C.M. Bishop et al. *Pattern recognition and machine learning*. Springer New York., 2006.
- [19] M.I. Jordan, Z. Ghahramani, T.S. Jaakkola, and L.K. Saul. An introduction to variational methods for graphical models. *Machine learning*, 37(2):183–233, 1999.
- [20] T. Kim, A. Chang, L. Holland, and A.S. Pentland. Meeting mediator: enhancing group collaboration using sociometric feedback. In *Proceedings of the ACM 2008 conference on Computer supported cooperative work*, pages 457–466. ACM, 2008.
- [21] A. Ahmed and E.P. Xing. Recovering time-varying networks of dependencies in social and biological studies. *Proceedings of the National Academy of Sciences*, 106(29):11878, 2009.
- [22] D. Schlangen. From reaction to prediction: Experiments with computational models of turn-taking. In *Ninth International Conference on Spoken Language Processing*. Citeseer, 2006.
- [23] J. Ginsberg, M.H. Mohebbi, R.S. Patel, L. Brammer, M.S. Smolinski, and L. Brilliant. Detecting influenza epidemics using search engine query data. *Nature*, 457(7232):1012–1014, 2008.
- [24] S.M. Siddiqi, B. Boots, and G.J. Gordon. A constraint generation approach to learning stable linear dynamical systems. *Advances in Neural Information Processing Systems*, 2007.
- [25] M. Shaw. *Group Dynamics: The Psychology of Small Group Behavior*. McGraw-Hill, 1976.
- [26] J.M. DiMicco, KJ Hollenbach, A. Pandolfo, and W. Bender. The Impact of Increased Awareness while Face-to-Face. *Human-Computer Interaction*, 22(1), 2007.
- [27] M.C. González, C.A. Hidalgo, and A.L. Barabási. Understanding individual human mobility patterns. *Nature*, 453(7196):779–782, 2008.

## 8 Appendix A: Model Learning

We here show detail steps for our variational E-M algorithm. Definition is denoted by  $\equiv$ , and  $\sim$  denotes the same distribution but the right side should be normalized accordingly.

### 8.1 E-Step

We adopt a procedure similar to the forward-backward procedure in HMM literature. We compute the following forward parameters for  $t = 1, \dots, T$ :

$$\alpha_{t,c}^{r_t} \equiv \text{Prob}(h_t^{(c)} | r_t, O_{1:t}), \quad (16)$$

$$\kappa_t \equiv \text{Prob}(r_t | O_{1:t}), \quad (17)$$

where  $O_{1:t}$  denotes  $\{O_{t'}^{(c)}\}_{t'=1, \dots, t}^{c=1, \dots, C}$ . However, exact inference is not intractable. We apply the variational approach in [14] [19]. The variational E-M process is still guaranteed to converge because of the lower bound property of the variational method [19]. We decouple the chains by:

$$\text{Prob}(h_t^{(1)}, \dots, h_t^{(C)} | O_{1:t}, r_t) \approx \prod_c Q(h_t^{(c)} | O_{1:t}, r_t), \quad (18)$$

and naturally:

$$\alpha_{t,c}^{r_t} \approx Q(h_t^{(c)} | O_{1:t}, r_t) \quad (19)$$

We define:

$$\alpha_{t,c} \equiv \text{Prob}(h_t^{(c)} | O_{1:t}) = \sum_{r_t} \kappa_t \alpha_{t,c}^{r_t}, \quad (20)$$

and

$$\widehat{\alpha}_{t-1,c}^{r_t} \equiv \text{Prob}(h_{t-1}^{(c)} | r_t, O_{1:t-1}) = \sum_{r_{t-1}} \widehat{\kappa}_{t-1}^{r_t} \alpha_{t-1,c}^{r_{t-1}}, \quad (21)$$

where:

$$\widehat{\kappa}_{t-1}^{r_t} = \text{Prob}(r_{t-1} | O_{1:t-1}, r_t). \quad (22)$$

We define  $Q(h^{(c)})$  to be in the form of  $\frac{\text{Prob}(h_t^{(c)} | O_{1:t-1}, r_t) s_t^{(c)}}{\sum_{h_t^{(c)}} \text{Prob}(h_t^{(c)} | O_{1:t-1}, r_t) s_t^{(c)}}$ , which captures

both the evidence from previous states ( $\text{Prob}(h_t^{(c)} | O_{1:t-1}, r_t)$ ) and the evidence ( $s_t^{(c)}$ ) from observations. We then have:

$$\begin{aligned} & Q(h_t^{(1, \dots, C)} | O_{1:t}, r_t) \\ & \left( \underbrace{\sum_{h_{t-1}^{(c)}} \mathbf{R}_{c,c}^{r_t} \mathbf{E}_{h_{t-1}^{(c)}, h_t^{(c)}}^{(c)} \widehat{\alpha}_{t-1,c}^{r_t} + \sum_{c', c' \neq c} \sum_{h_{t-1}^{(c')}} \mathbf{R}_{c,c'}^{r_t} \mathbf{F}_{h_{t-1}^{(c')}, h_t^{(c)}}^{(c')} \widehat{\alpha}_{t-1,c'}^{r_t}}_{\Psi^{(c)}} \right) \times s_t^{(c)} \\ & \equiv \prod_c \frac{\left( \sum_{h_{t-1}^{(c)}} \mathbf{R}_{c,c}^{r_t} \mathbf{E}_{h_{t-1}^{(c)}, h_t^{(c)}}^{(c)} \widehat{\alpha}_{t-1,c}^{r_t} + \sum_{c', c' \neq c} \sum_{h_{t-1}^{(c')}} \mathbf{R}_{c,c'}^{r_t} \mathbf{F}_{h_{t-1}^{(c')}, h_t^{(c)}}^{(c')} \widehat{\alpha}_{t-1,c'}^{r_t} \right) \times s_t^{(c)}}{\sum_{h_t^{(c)}} \left( \sum_{h_{t-1}^{(c)}} \mathbf{R}_{c,c}^{r_t} \mathbf{E}_{h_{t-1}^{(c)}, h_t^{(c)}}^{(c)} \widehat{\alpha}_{t-1,c}^{r_t} + \sum_{c', c' \neq c} \sum_{h_{t-1}^{(c')}} \mathbf{R}_{c,c'}^{r_t} \mathbf{F}_{h_{t-1}^{(c')}, h_t^{(c)}}^{(c')} \widehat{\alpha}_{t-1,c'}^{r_t} \right) \times s_t^{(c)}} \quad (23) \end{aligned}$$

where  $\Psi^{(c)}$  is actually  $\text{Prob}(h_t^{(c)}|O_{1:t-1}, r_t)$ . We also have:

$$\text{Prob}(h_t^{(1,\dots,C)}, O_t|O_{1:t-1}, r_t) = \prod_c \underbrace{\left( \sum_{h_{t-1}^{(c)}} \mathbf{R}_{c,c}^{r_t} \mathbf{E}_{h_{t-1}^{(c)}, h_t^{(c)}}^{(c)} \widehat{\alpha}^{r_t}_{t-1,c} + \sum_{c', c' \neq c} \sum_{h_{t-1}^{(c')}} \mathbf{R}_{c,c'}^{r_t} \mathbf{F}_{h_{t-1}^{(c')}, h_t^{(c)}}^{(c')} \widehat{\alpha}^{r_t}_{t-1,c'} \right)}_{\Psi^{(c)}} \text{Prob}(O_t^{(c)}|h_t^{(c)}), \quad (24)$$

and

$$\text{Prob}(h_t^{(1,\dots,C)}|O_{1:t-1}, r_t) = \frac{\text{Prob}(h_t^{(1,\dots,C)}, O_t|O_{1:t-1}, r_t)}{\text{Prob}(O_t|O_{1:t-1}, r_t)}. \quad (25)$$

We continue to minimize the K-L divergence between  $\text{Prob}(h_t^{(1,\dots,C)}|O_{1:t}, r_t)$  and  $Q(h_t^{(1,\dots,C)}|O_{1:t}, r_t)$ , that is:

$$\begin{aligned} \arg \min_{s_t^{(c)}} \mathbb{D} &\equiv \mathbb{E}_Q \left( \log Q(h_t^{(1,\dots,C)}|O_{1:t}, r_t) \right) - \mathbb{E}_Q \left( \text{Prob}(h_t^{(1,\dots,C)}|O_{1:t}, r_t) \right) \\ &= \mathbb{E}_Q \left( \sum_c \log \Psi^{(c)} + \sum_c \log s_t^{(c)} - \sum_c \log \left( \sum_{h_t^{(c)}} \Psi^{(c)} s_t^{(c)} \right) \right) \\ &\quad - \mathbb{E}_Q \left( \sum_c \log \Psi^{(c)} + \sum_c \log \text{Prob}(O_t^{(c)}|h_t^{(c)}) \right) + \underbrace{\text{Prob}(O_t|O_{1:t-1}, r_t)}_{\text{unrelated to } s_t^{(c)}} \end{aligned} \quad (26)$$

By taking the derivative we have:

$$\begin{aligned} \frac{\partial \mathbb{D}}{\partial s_t^{(c)}} &= \sum_{h_t^{(c)}} \frac{\partial \widehat{\alpha}^{r_t}_{t,c}}{\partial s_t^{(c)}} \left( s_t^{(c)} - \text{Prob}(O_t^{(c)}|h_t^{(c)}) \right) = 0 \\ &\Rightarrow s_t^{(c)} = \text{Prob}(O_t^{(c)}|h_t^{(c)}) \end{aligned} \quad (27)$$

We then compute  $\kappa_t$  using Bayes' rule:

$$\kappa_t \sim \text{Prob}(O_t|r_t, O_{1:t-1})\text{Prob}(r_t|O_{1:t-1}). \quad (28)$$

where  $\text{Prob}(O_t|r_t, O_{1:t-1})$  can be evaluated using the previous approximation results. The prior part of Eq. 28 can be evaluated using  $\mathbf{V}$  and  $\kappa_{t-1}$ .

Using the same idea, we can compute the following backward parameters for all  $t$ :

$$\beta_{t,c}^{r_t} \equiv \text{Prob}(h_t^{(c)}|r_t, O_{t:T}), \quad (29)$$

$$\nu_t \equiv \text{Prob}(r_t|O_{t:T}), \quad (30)$$

$$\beta_{t,c} \equiv \text{Prob}(h_t^{(c)}|O_{t:T}) = \sum_{r_t} \nu_t \beta_{t,c}^{r_t}. \quad (31)$$

## 8.2 M-step

With  $\kappa_t$  and  $\nu_t$ , we can estimate:

$$\xi_{i,j}^t \equiv \text{Prob}(r_t = i, r_{t+1} = j | O_{1:T}) = \frac{\text{Prob}(r_t = i | O_{1:t}) \text{Prob}(r_{t+1} = j | O_{t+1:T}) \text{Prob}(r_{t+1} | r_t)}{\sum_{i,j} \text{Prob}(r_t = i | O_{1:t}) \text{Prob}(r_{t+1} = j | O_{t+1:T}) \text{Prob}(r_{t+1} | r_t)}, \quad (32)$$

and

$$\lambda_i^t = \text{Prob}(r_t = i | O_{1:T}) = \frac{\sum_j \xi_{i,j}^t}{\sum_i \sum_j \xi_{i,j}^t}. \quad (33)$$

We then update  $V$  by:

$$\mathbf{V}_{i,j} \leftarrow \frac{\sum_t \xi_{i,j}^t + k}{\sum_t \sum_j \xi_{i,j}^t + p^V}, \quad (34)$$

where  $k = p^V$  if  $i = j$ , 0 otherwise.

We compute the following joint distribution.

$$\text{Prob}(h_t^{(c)}, h_{t+1}^{(c)}, q_{t+1}^{(c)}, r_{t+1} | O_{1:T}) = \begin{cases} \frac{1}{Z} T_{h_t^{(c)}, h_{t+1}^{(c)}}^{(c)} \times \widehat{\alpha}_{t,c}^{r_t} \beta_{t+1,c}^{r_t} \lambda^t \text{Prob}(q_{t+1}^{(c)} | r_{t+1}), & \text{if } q_{t+1}^{(c)} = c, \\ \frac{1}{Z} F_{h_t^{(c)}, h_{t+1}^{(c)}}^{q_{t+1}^{(c)}} \times \widehat{\alpha}_{t,q_{t+1}^{(c)}}^{r_t} \beta_{t+1,c}^{r_t} \lambda^t \text{Prob}(q_{t+1}^{(c)} | r_{t+1}), & \text{if } q_{t+1}^{(c)} \neq c. \end{cases} \quad (35)$$

$Z$  denotes the normalization factor that can be calculated easily by summing all possible values for each variable. This is fast to compute since the joint distribution is made of only four variables. By marginalizing Eq. 35, we can update parameters  $\mathbf{R}$ ,  $\mathbf{E}$  and  $\mathbf{F}$ :

$$\mathbf{R}_{c_1, c_2}^j \leftarrow \frac{\sum_t \text{Prob}(q_t^{(c_1)} = c_2, r_t = j | O_{1:T})}{\sum_t \sum_c \text{Prob}(q_t^{(c_1)} = c, r_t = j | O_{1:T})}, \quad (36)$$

$$\mathbf{E}_{s_i, s_j}^{(c)} \leftarrow \frac{\sum_t \text{Prob}(h_t^{(c)} = s_i, h_{t+1}^{(c)} = s_j, q_t^{(c)} = c | O_{1:T})}{\sum_t \sum_s \text{Prob}(h_t^{(c)} = s_i, h_{t+1}^{(c)} = s, q_t^{(c)} = c | O_{1:T})}, \quad (37)$$

and

$$\mathbf{F}_{s_i, s_j}^{(c)} \leftarrow \frac{\sum_t \sum_{c'} \text{Prob}(h_t^{(c)} = s_i, h_{t+1}^{(c')} = s_j, q_{t+1}^{(c')} = c | O_{1:T})}{\sum_t \sum_{c'} \sum_s \text{Prob}(h_t^{(c)} = s_i, h_{t+1}^{(c')} = s, q_{t+1}^{(c')} = c | O_{1:T})}. \quad (38)$$

## 9 Appendix B: Detecting Structural Changes in the Discussion Dynamics

We here provide an additional example for detecting structural changes using the same dataset described in Section 5 of our paper.

One important feature of this model is its ability to capture changes in influence dynamics given only observed time series for each node. In this section, we will demonstrate the performance of our model in detecting changes with the group discussion dataset.

In our discussion, a *sample* refers to the set of four sequences collected by the four badges in deployed in a group discussion session. We adopt the following evaluation procedure: One mixed binary audio sample for each four-person group is generated by concatenating the co-located discussion session sample and the distributed discussion session sample of the same group. It is known that [20] the interaction pattern in a distributed discussion session is often different from a co-located discussion session. Therefore, we are able to create ground truth about changes of influence patterns by switching from a distributed discussion sample to a co-located discussion sample manually. It should be noted that we only use binary sequences by thresholding the volume variance. Thus, we have eliminated all information in the audio content. Two samples from each group are included in our final evaluation set: a) the original sample of the co-located discussion session (CO) and b) the mixed sample as described above (CO+DS). We end up with a total of 28 groups and 56 samples in the final set. Lengths of each sample vary from 100 seconds to 500 seconds.

We apply our model on both samples for each group. The emission probability in our model is used to tolerate possible error due to hard thresholding and possible noise. We choose  $J = 2$ , and  $p^V$  is optimized for best performance. The posterior of  $r^t$  for the two samples from each group is stored as the output of the algorithm.

We continue to develop simple heuristics for distinguishing DS+CO from CO by looking at the difference of the expected influence matrix ( $\sum_j \lambda_j^t R_j$ ) at  $t = 1$  and  $t = 0.8T$  for each sample, and the one with larger difference is labeled as the CO+DS sequence. Given the pair of samples for each group, we test the labeling accuracy based on the output of our model. For comparison, we also implement two other techniques: a) classification based on one single feature, the turn taking rate, and b) S.V.M.-based classification (using implementation in [?]). It is well recognized that the turn taking rate is an important indicator for group dynamics. We compute the two turn taking rates for each pair of samples and compare them to determine sample labels. For S.V.M., we compute the turn taking rate and the speaking durations for each group member as the feature vector for each sample. Its performance is obtained via a four-fold cross validation. It should be emphasized that the S.V.M. classification task is different from the other two, and it is naturally more challenging: all samples are mixed together before fed to S.V.M. rather than being fed to other two algorithms in a pairwise manner.

We must point out that the ground truth in our evaluation may not be accurate: There is no guarantee in the dataset that a group of people behave and interact with each other differently when they are performing discussions using remote communication tools rather than being in the same room.

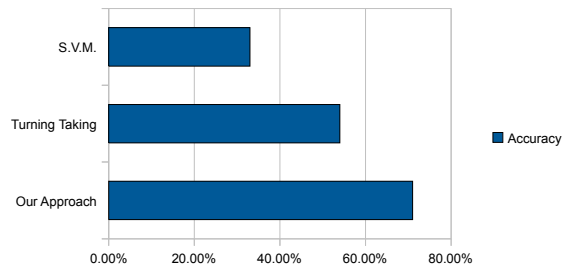


Figure 4: The accuracy rates for classifying CO+DS samples from CO samples are shown above. Our algorithm performs significantly better than the other two methods, which are based on simple statistical features.

We illustrate the accuracy rates in Fig. 4. As we expected, our algorithm reaches 71% accuracy and outperforms the other two methods. We argue that the influence dynamic is an intrinsic property of the group, which can not be fully revealed using simple statistical analysis on observable features. To investigate and visualize the dynamical characteristics of human interaction patterns, a more sophisticated model, such as our dynamical influence process, must be deployed to reveal the subtle differences in influence dynamics.

In addition, we claim that our model is capable of modeling, quantifying and tracking occurrences of such shifts in face-to-face dynamics accurately. Our model fits its parameters to best suit switches between different influence patterns, and the parameters will be helpful for sociologists to objectively investigate the micro relationship in a group discussion session. Information discovered by our algorithm will also be useful in applications such as understanding possible interventions in human interactions[20][26].